Structure of Proton-Conducting Anhydrous Gel Electrolytes Based on Poly(glycidyl methacrylate)

Grazyna Z. Zukowska,*,† Valerie J. Robertson,† Marek L. Marcinek,‡ Kenneth R. Jeffrey,† and James R. Stevens†

The Guelph-Waterloo Physics Institute, Department of Physics, University of Guelph, Guelph, Ontario, Canada N1G 2W1, and Warsaw University of Technology, Faculty of Chemistry, Noakowskiego 3, 00-664 Warszawa, Poland

Received: February 19, 2003

In the past few years, considerable effort has been put into the development of stable proton-conducting systems consisting of a strong acid dissolved in a solvent entrapped in a polymer gel. There has been continuing interest in orthophosphoric acid dissolved in aprotic solvents such as propylene carbonate (PC) and *N,N*-dimethyl formamide (DMF), which are contained in methacrylate-based polymer gels. In this report, we present the results of a study of those phosphoric acid−solvent−methacrylate-based polymer gel electrolytes that have ionic conductivities above 5×10^{-4} S·cm^{-1} at ambient temperature. FT-IR, FT-Raman, and high-resolution NMR spectroscopies are used. The objective is to understand better the interaction of orthophosphoric acid with the solvent and the polymer gel to gain information on possible proton-conduction mechanisms.

1. Introduction

Gel electrolytes, which are characterized by both high conductivity and good mechanical properties, have been intensively studied as prospective materials for lithium batteries, fuel cells, humidity sensors, and electrolytes for electrochromic devices.[1,2] Proton-conducting systems seem to be particularly suitable for electrochromic applications because of the high mobility of protons resulting in high conductivity at ambient temperature. Pioneering work by Lassegues[1] and Kreuer[3] is particularly notable.

In previous studies, several types of gels doped with orthophosphoric acid were investigated.[4−9] Properties of those systems were strongly affected by the type of solvent and by the polymer matrix. The poly(methyl methacrylate) (PMMA)−PC−H$_3$PO$_4$-based systems were characterized by increasing conductivity with rising acid concentration, whereas for the poly(glycidyl methacrylate) (PGMA)−DMF−H$_3$PO$_4$ system the maximum in conductivity occurred at about 7 wt % of the incorporated acid.[4,7] The differences between these types of gels are a result of (i) the lower dielectric constant of DMF as compared to that of PC and therefore the formation of ion pairs in the former and (ii) the reaction of phosphoric acid with the glycidyl group of the polymer, leading to additional cross linking of the system. The half-esters of phosphoric acid, formed in the reaction of its addition to the oxirane ring, are stronger acids than H$_3$PO$_4$ and are responsible for higher conductivities in the gel samples as compared to those of their liquid analogues with the same acid content.

In the present work, a more precise analysis of the structure of the polymer matrix and its interactions with a solvent is undertaken. On the basis of high-resolution ^{31}P NMR and ^{1}H NMR as well as ^{1}H−^{31}P NMR heteronuclear total correlation spectroscopy (hetero-TOCSY)[10] experiments, the approximate amounts of different phosphate species (i.e., cyclic phosphates, monoesters, diesters, etc.) obtained during the gel synthesis were estimated. A comparison of the ^{31}P NMR spectra of the gel and liquid samples leads to the conclusion that both the gel and liquid samples with high (above 20 wt %) acid content contain condensed phosphates (e.g., pyrophosphoric and triphosphoric acids). Using both Raman and FT-IR spectroscopies, we analyzed the influence of the acid concentration on the formation of hydrogen bonds linking acid and solvent molecules. We also considered the changes in the acid−solvent interactions with and without the presence of a polymer matrix.

2. Experimental Section

2.1. Materials. DMF (Aldrich, anhydrous), perdeuterated DMF (DMF-d_7, 95% D, Cambridge Isotope), and GMA (Aldrich, reagent grade) were used without further purification. Benzoyl peroxide (Aldrich, 70%) was recrystallized from chloroform and dried under vacuum. H$_3$PO$_4$ (Aldrich, 98% crystals) was used as received.

2.2. Sample Preparation. Nonaqueous protonic gels were prepared in small glass reactors. Initially, H$_3$PO$_4$ was dissolved in a solvent (DMF). Gels used for proton NMR experiments were swollen with DMF-d_7. The monomer and a free-radical initiator (benzoyl peroxide) were then added, and the mixture was stirred to obtain a homogeneous solution in an argon-filled drybox (moisture content below 10 ppm). Each of the mixtures was heated to 75 °C for 4−24 h to form a gel.

Gels containing more than 7 wt % of the acid were colorless and transparent, and the sample with the lowest (3 wt %) acid content was yellowish and slightly opaque.

In the preparation of samples for 2D hetero-TOCSY and COSY experiments, an appropriate amount of orthophosphoric acid was dissolved in DMF-d_7; monomer was then added. These solutions were put into NMR vials and kept at 75 °C for approximately 6 h.

* Corresponding author. E-mail: zosia@chemix.ch.pw.edu.pl or zosia@helios.physics.uoguelph.ca. Fax 01-519-836-9967.
† University of Guelph.
‡ Warsaw University of Technology.

Glycidyl Methacrylate. ^{1}H NMR δ: 6.103 (s, 1H, H$_{a1}$), 5.725 (s, 1H, H$_{a2}$), 4.505−4.508 (dd, 1H, H$_{c1}$), 3.988−3.941 (dd, 1H, H$_{c2}$), 3.301−3. 261 (m, 1H, H$_d$), 2.853−2.83 (t, 1H, H$_{e1}$), 2.723−2.704 (dd, 1H, H$_{e2}$), 1.930 (s, 3H, H$_b$).

2-Methyl-acrylic acid-2-hydroxy-2-oxo-2λ^5-[1,2,3]dioxaphospholan-4-yl methyl ester (1). ^{1}H NMR δ: 6.087 (s, 1H, H$_{a1}$), 5.661 (s, 1H, H$_{a2}$), 4.6−4.38 (dd, 1H, H$_{c1}$), 4.35−4.327 (dd, 1H, H$_{e1}$), 4.264−4.235 (dd, 1H, H$_{e2}$), 4.067−4.0239 (dd, 1H, H$_{c2}$), 1.894 (s, 3H, H$_b$). ^{31}P NMR δ: 17.6

2-Methyl-acrylic acid-2-hydroxy-3-phosphonoxy-propyl ester (2a). ^{1}H NMR (only signals of H$_c$, H$_d$, H$_e$ listed) δ: 4.21−4.18 (dd, 1H, H$_{c1}$), 4.15−4.12 (dd, 1H, H$_{c2}$), and 3.72−3.68 (m, 1H, H$_d$). ^{31}P NMR δ: 1.26

2-Methyl-acrylic acid 2-[2-hydroxy-3-(2-methyl-acryloyl-oxy)-propoxy]-2-oxo- 2λ^5-[1,3,2]dioxaphospholan-4-ylmethyl ester (3). ^{1}H NMR δ: 4.70−4.64 (weak, m), 4.52 (weak, m), 4.91−4.71 (medium, dd), 4.46−4.24 (medium, m), 4.39−4.37 (medium, m), 4.21−4.17 (strong, m), 4.11−4.08 (weak, dd or m). ^{31}P NMR δ: 17.3

3. Experimental Techniques

3.1. NMR Spectroscopy. NMR spectra were generally run in DMF-d_7 at 300 K on Bruker Avance spectrometers operating at either 400 or 600 MHz for protons. Proton and hetero-TOCSY spectra were collected using either a broad-band inverse dual probehead (Avance 400) or a triple-resonance inverse probehead (Avance 600). ^{31}P NMR spectra were recorded on a Bruker Avance-600 spectrometer using a broad-band observed probehead at 242.9 MHz. ^{1}H NMR chemical shifts are reported in δ relative to external TSP (sodium 3-(trimethylsilyl)propionate-d_4). ^{31}P NMR chemical shifts are reported in δ downfield (+) and upfield (−) from an external standard consisting of 85% H$_3$PO$_4$. Acquisition parameters included the following. 1D spectra: 32K data points were collected with a 12 (^{1}H) or 100 (^{31}P) ppm sweep width and a 301 flip angle, apodized with 0.1-Hz line broadening and zero filled to 64K before Fourier transformation. A 1.5-s recycle delay was employed. [31]P spectra were broad-band proton decoupled. 2D COSY: 2K data points were collected for each of 256 increments. The recycle delay was 1 s, and a sinebell window function was applied in both the t$_1$ and t$_2$ domains following zero filling to 512K in the t$_1$ domain. Two-dimensional hetero-TOCSY: 2K data points were collected for each of 1024 increments. Spectra were recorded with a spectral width of 5681 Hz in F2 and 12 136 Hz in F1 with 16 transients per increment. To saturate the protons, 180 decoupler pulses were applied with an interpulse delay of 50 ms for a period of 2 s. A DIPSI-2 sequence was used for spin locking with low-power 90° pulses of 40 μs calibrated for both ^{1}H and ^{31}P channels. Trim pulses (2.5 ms each) were applied before and after the spin-lock period. Phase-sensitive detection was achieved using the time-proportional phase incrementation method (TPPI). Data were apodized using sinebell squared window functions in both dimensions.

The assignment of the lines in the NMR spectra is based on literature data,[11−17] 2D [1]H−^{1}H COSY, and [1]H−[31]P hetero-TOCSY experiments.

3.2. FT-IR. Infrared absorption spectra were recorded on a computer-interfaced Nicolet Nexus 870, which has a resolution of 2 cm^{-1} in the range of 4000 to 600 cm^{-1}. FT-IR studies were performed at 25 °C, and the electrolyte samples were sandwiched between two NaCl plates.

3.3. Raman Spectroscopy. Raman spectra were recorded using a Renishaw System 2000 Raman spectrometer equipped with a confocal Raman microscope, a 1200 lines/mm holo-graphic grating, and a CCD camera. An argon laser operating at 514 nm was used as the excitation source, and the spectral resolution was about 2 cm^{-1}. To avoid contact with air during the measurements, samples were kept in sealed glass cuvettes.

4. Results and Discussion

4.1. NMR Studies. It is known that epoxides can react with H$_3$PO$_4$ either by the phosphorylation of the epoxide ring or by its ionic polymerization,[11−13] as shown in Scheme 1. Studies of Raducha et al.[3] revealed the presence of both kinds of products from this reaction. To understand the structure of the resulting adducts better as well as to obtain some information on the rate of H$_3$PO$_4$ consumption, we have studied the ^{1}H NMR and ^{31}P NMR spectra for the reaction mixture of H$_3$PO$_4$ and GMA in DMF-d_7. Increased viscosity in some samples resulted in significant line broadening in both ^{1}H and ^{31}P NMR spectra, making it difficult to observe signals of all of the ester species present in the polymer gels. In addition, the complexity of the 1D spectra made straightforward assignments impossible. The 2D hetero-TOCSY[10] experiment is ideally suited to the study of complex mixtures of phosphorylated moieties. In this experiment, individual phosphorus resonances are correlated to their proton neighbors and then to remaining protons in a *J*-coupled pathway during a period of spin locking. Data from this experiment together with the COSY and 1D information was used to estimate the distribution of the main products formed by monomeric GMA and H$_3$PO$_4$ in DMF-d_7.

Phosphorus Spectra. The ^{31}P NMR studies permit some conclusions about the structure of the polymer gel matrix itself as well as the ratio of the nonbonded phosphoric acid and phosphoric acid esters. It is known that in concentrated solutions phosphoric acid exists in equilibrium with chain phosphates.[14] A comparison of the spectra of PGMA−H$_3$PO$_4$−DMF polymer gels and GMA−H$_3$PO$_4$−DMF solutions (Figures 1a and 1b) and DMF−H$_3$PO$_4$ solutions clearly indicates the presence of pyrophosphoric acid and triphosphoric acid in these electrolytes. Here, the concentration of the condensed phosphates increases with increase in acid content. The concentration of pyrophosphoric acid is higher for polymer gel samples than for the liquid electrolytes with the same acid content. In our opinion, this can be caused by the relatively lower dielectric constant of the plastified polymer gel (less-polar polymer) as compared to that of DMF itself. We also observed differences in the chemical shift of the strongest signals, those of orthosphosphoric acid and pyrosphophoric acid, as compared to that of the external standard. This is probably caused by DMF−acid interaction, which is discussed below in section 4.3. The chemical shift of H$_3$PO$_4$ depends on the acid concentration; changes are 0.536, 1.598, and 2.271 ppm for samples containing 40, 20, and 7 wt % acid, respectively. The interactions between the solvent and the acid are also distinctly shown in the ^{1}H NMR spectra of DMF−H$_3$PO$_4$ solutions, where all of the signals of the solvent are shifted toward higher δ values as the acid concentration increases.

In the spectra of gel electrolytes, one can observe, besides signals of linear phosphates, broader and weaker peaks with maxima at δ 1.3 and ~17.6. The first of these signals we assign to the linear monoesters of the phosphoric acid, and the second, to the cyclic phosphates. The ratio of intensities of both of these peaks to the intensity of the main peak ascribed to the orthophosphoric acid is the highest for the sample with the lowest acid concentration (3 wt %). The distribution of these distinct species for the gel samples is presented in Table 1.

Conversion of the Epoxide. As mentioned above, the oxirane ring can react with the P−OH group of the phosphoric acid

Structure of Proton-Conducting Gel Electrolytes

J. Phys. Chem. B, Vol. 107, No. 24, 2003 **5799**

SCHEME 1: Structure of Glycidyl Methacrylate and Products of Its Reaction with Phosphoric Acid
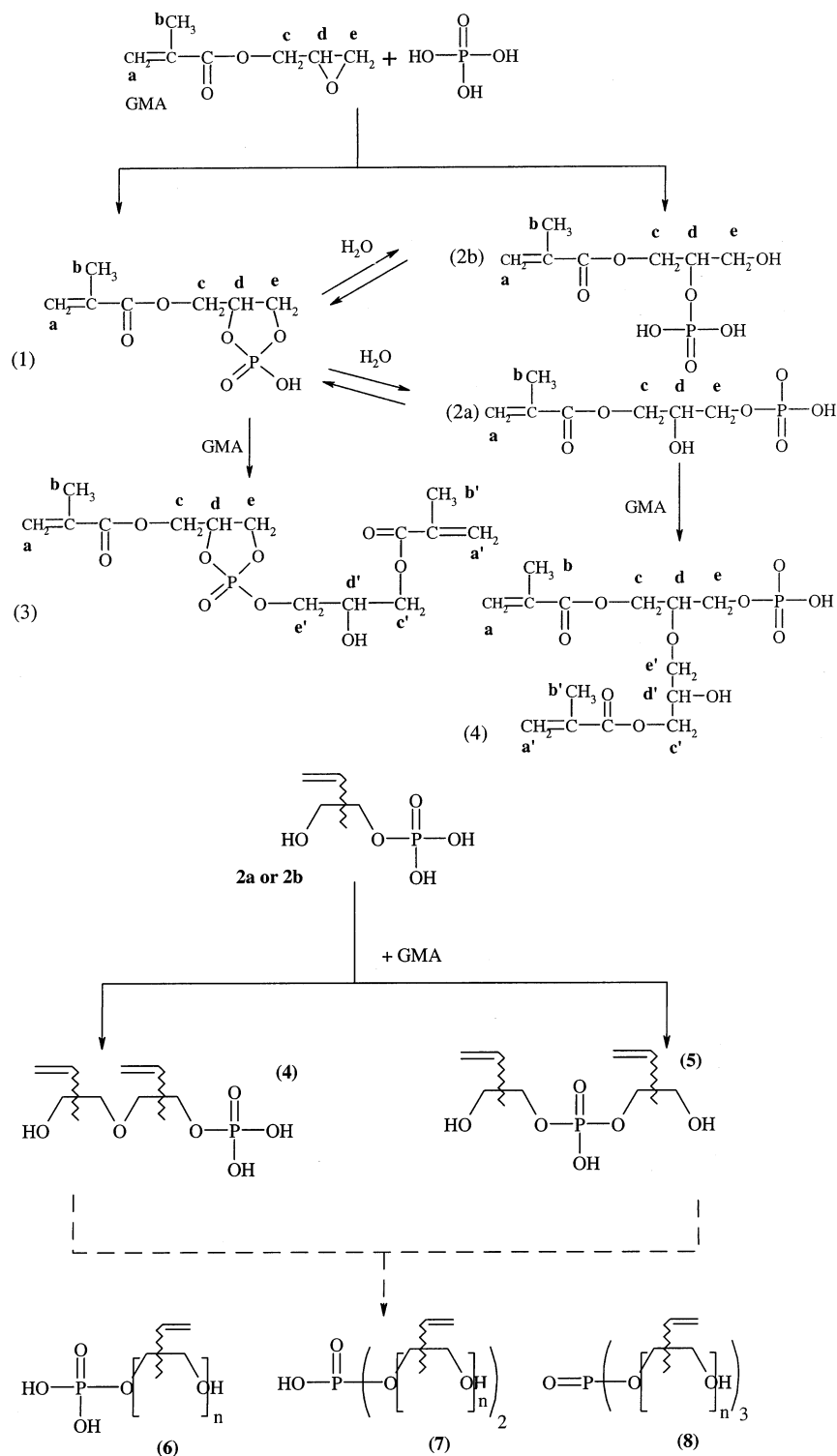
(and its mono- or diesters), leading to the formation of species containing both P—OH and C—OH groups. This is followed by the addition reaction of the oxirane ring with C—OH groups according to the so-called "activated monomer mechanism". This results in a mixture of phosphorus-containing oligoethers with unsaturated bonds in the side chains. In the presence of benzoyl peroxide, the oligoethers can polymerize via side-chain double bonds, thus forming cross-linked structures. The analysis of the ^{1}H NMR spectra of the gel samples was difficult because of the broadening of the NMR signals; we decided, therefore, to concentrate our measurements on the GMA—H_3PO_4 adducts

in solution in DMF-d_7. A comparison of ^{1}H NMR spectra taken at 75 °C after 0.5, 2, and 5 h (Figure 2) clearly shows a decrease in the intensity of the multiplets δ 3.29–3.25, 2.84–2.82, and 2.71–2.69, which are attributed to the CH and CH_2 protons of the oxirane ring. Figure 3 shows the reaction conversion curve for GMA to its adducts, which is estimated on the basis of the intensity of the signal from the proton of the CH group to that of the methyl protons. During the time of the reaction, several new groups of multiplets can be observed. For example, there are multiplets between 4.25 and 4 ppm, a doublet at 3.58–3.56 ppm, and multiplets at 3.74–3.72 and 3.88–3.86
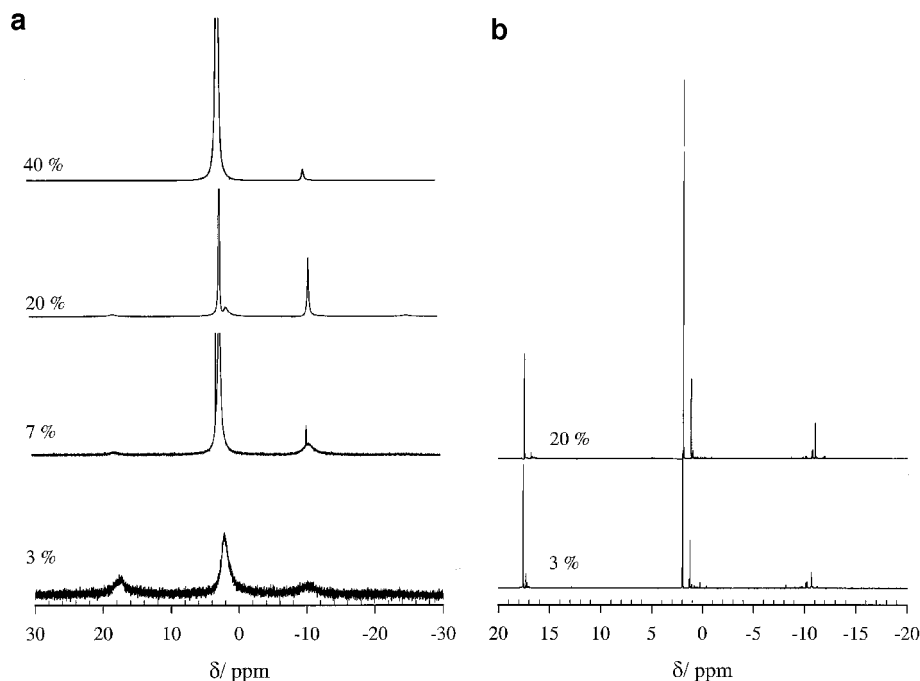
Figure 1. Comparison of ^{31}P NMR spectra of the (a) PGMA$-$H$_3$PO$_4$$-$DMF and (b) GMA$-H_3PO_4$$-$DMF samples. Acid content is equal to (a) 3, 7, 20, and 40 wt % or (b) 3 and 20 wt %.
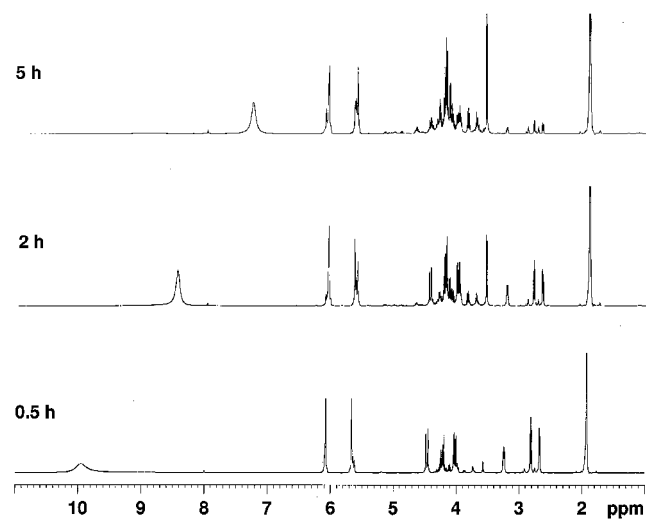

Figure 2. ^{1}H NMR spectra of the products of the reaction between GMA and H$_3$PO$_4$ in DMF-d_7 after 0.5, 2, and 5 h. The reaction was carried out in an NMR tube at 75 °C for 5 h. Acid content was equal to 7.2 wt %, and the GMA/H$_3$PO$_4$ molar ratio was 1.1.

TABLE 1: Percentage of Phosphate Species Present in PGMA$-$DMF$-$H$_3$PO$_4$ Polymer Gels[a]

acid content/ wt %	cyclic phosphates	(H$_3$PO$_4$)	(monoesters)	H$_4$P$_2$O$_7$	H$_5$P$_3$O$_{10}$
3	47.4	52.6			
7	7.9	12.4	75.1	4.6	
20	1.7	75.8	7.4	14.4	0.7
40	0.4	87	5.6	6.9	0.1

[a] Estimation based on ^{31}P NMR data analysis.

ppm. Much weaker groups of signals appeared between 4.6 and 5.3 ppm.

Another characteristic change in the proton spectrum, observed in the course of the reaction, is the shift of the signal for mobile protons from 10.6 ppm, which is typical for acid, to 7.3 ppm (Figure 2). This indicates the creation of alcohol-type hydroxyl groups and hence the presence of an averaged signal
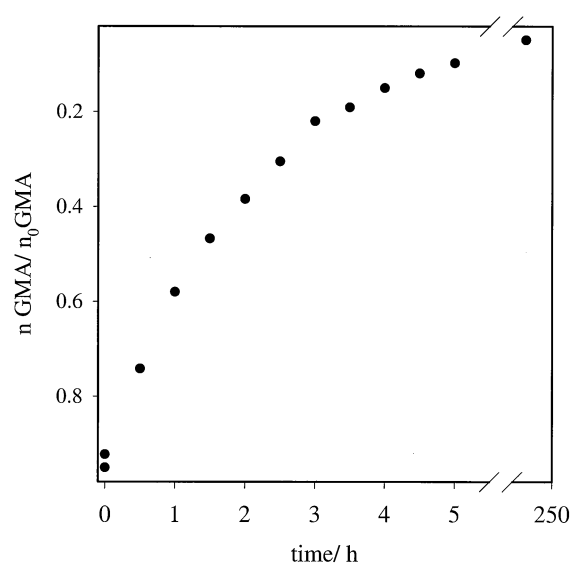

Figure 3. Conversion-time curve corresponding to the overall conversion of epoxy groups in the reaction between GMA and H$_3$PO$_4$ at 75 °C in DMF-d_7 (by ^{1}H NMR).

due to the rapid exchange of protons between C$-$OH and P$-$OH hydroxyl group.

Idendification of the Reaction Products: TOCSY and COSY Spectra. ^{31}P NMR spectra show peaks between 18 and 17 ppm, at 2.4 ppm, and numerous signals between 1.6 and -0.4, -8.2 and -10.5, and -23.2 and -24 ppm. On the basis of literature data[11$-$17] and 2D hetero-TOCSY spectra (Figure 4 a and b), the lowest-field signals were assigned to cyclic phosphates, the strong peak at 2.4 ppm (not coupled with any protons), to H$_3$PO$_4$, signals between 1.6 and -0.4 ppm, to various mono-, di-, and triesters of phosphoric acid, peaks between -8.2 and -10.5 ppm, to pyrophosphoric acid and its esters, and the lines in the range between -23.2 and -24 ppm, to triphosphoric acid. The proportion of each phosphate species depends on the acid/GMA ratio. In the TOCSY spectrum of the sample with lowest acid content (3 wt %) (Figure 4a), cross
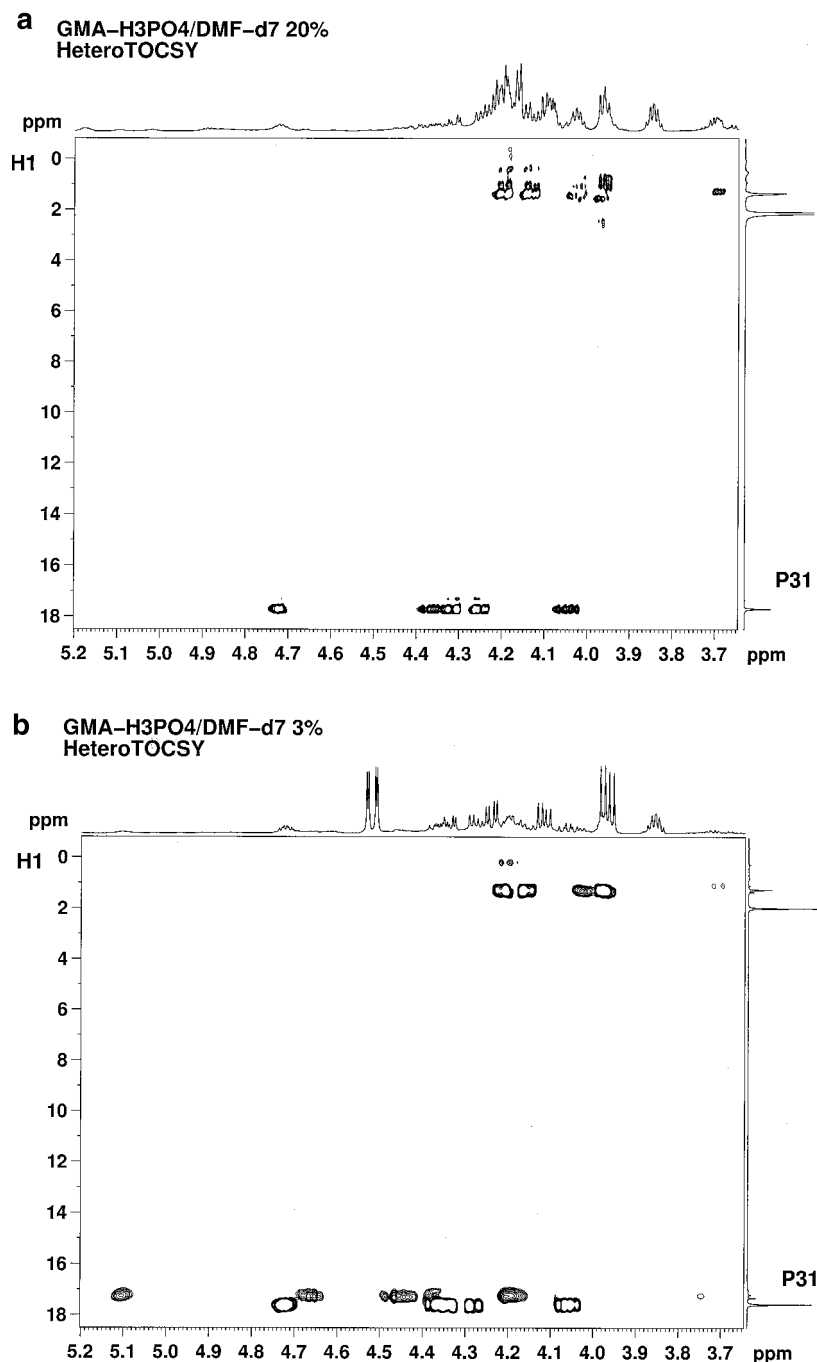
Structure of Proton-Conducting Gel Electrolytes

J. Phys. Chem. B, Vol. 107, No. 24, 2003 **5801**

Figure 4. 2D $^1H-^{31}P$ NMR TOCSY spectrum of the reaction mixture of GMA and H_3PO_4 in DMF-d_7. Acid content was equal to (a) 3 and (b) 20 wt % with respect to DMF.

peaks of four main products can be distinguished. Two of these products are identified as cyclic compounds **1** and **3**, and two others are linear monoesters of phosphoric acids, most probably **2a** and **4** (see Scheme 1).

In the ^{31}P NMR spectra, compounds **1** and **3** absorb at 17.6 and 17.3 ppm, which clearly indicates that these compounds are five-membered cyclic phosphates. Cross peaks seen in the hetero-TOCSY spectrum (corresponding to **1**) come from a correlation of the phosphate with the H_c, H_d, and H_e protons of the ester. From the analysis of the cross section in Figure 4a, we can distinguish the following groups of signals: two doublets of doublets at δ 4.35−4.327 and 4.264−4.235, two weaker doublets of doublets at δ 4.067−4.024 and 4.38−4.36, and a multiplet at δ 4.72−4.71. Signals resonating at δ 4.35−4.327 and 4.264−4.235 are the most intense; we attribute them to H_e

protons. The multiplet corresponds to the methine proton H_d, and two weaker doublets of doublets, to methylene protons H_c.

Phosphorus nuclei resonating at 1.26 ppm give cross peaks coming from a correlation with protons absorbing at 4.21−4.18 ppm, 4.15−4.12 ppm, and 3.72−3.68 ppm. The intensity of the two former signals, which are both doublets of doublets, is much higher than that of the latter (multiplet). We therefore conclude that this compound is a linear monoester, most probably **2a**. These groups of signals correspond respectively to H_c (3.72−3.68 ppm) and H_d (4.21−4.18 and 4.15−4.12 ppm) protons. Signals of the H_e protons are probably too weak to give a cross peak.

Phosphorus nuclei absorbing at 17.3 ppm give at least seven cross-peaks in the hetero-TOCSY spectrum. The higher number of cross peaks as well as a decrease in the chemical shift suggest
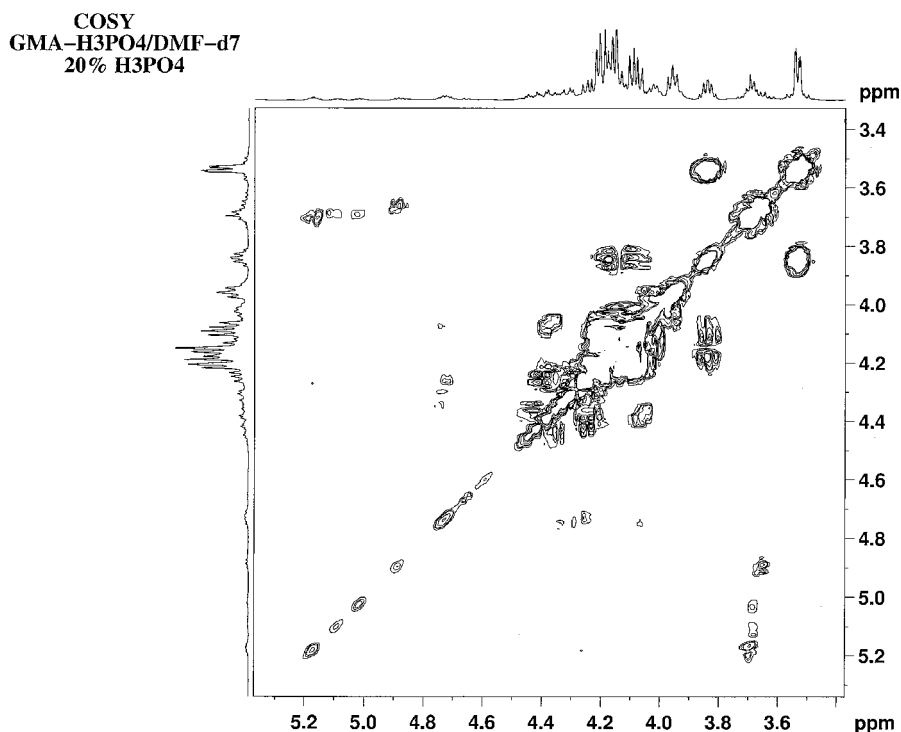
Figure 5. 2D ^{1}H$-$^{1}H NMR COSY spectrum of the reaction mixture of GMA and H$_3$PO$_4$ in DMF-d_7. Acid content was equal to 20 wt % with respect to DMF.

that this signal might correspond to the cyclic ester with structure **3** (i.e., the product of the reaction of **1** with an another molecule of GMA). This cross section is blurred, but it is still possible to observe the following groups of signals: δ 4.70$-$4.64 (weak, m), 4.52 (weak, m), 4.91$-$4.71 (medium, dd), 4.46$-$4.24 (medium, m), 4.39$-$4.37 (medium, m), 4.21$-$4.17 (strong, multiplet), 4.11$-$4.08 (weak, m or dd). Some of these signals (e.g., the multiplet at 4.21$-$4.17 ppm) have the same chemical shifts as signals of **2a**, which indicates that they correspond to the H$_{c'}$, and H$_{d'}$ protons of compound **3**.

The analysis of the proton spectra permits a rough estimation of the ratio of products of the addition reaction of H$_3$PO$_4$ (i.e., ester species) to the products of the oligomerization of glycidyl methacrylate. According to the hetero-TOCSY experiments, the following multiplets are observed in ^{1}H NMR spectrum: δ 3.58$-$3.56, 3.88$-$3.86, and $\sim$ 4.1 show no coupling with any phosphorus signals. This suggests the formation of the products of the C$-$OH addition. From the analysis of the ^{1}H$-$^{1}H COSY spectrum (Figure 5), we conclude that this adduct corresponds to structure **4** in Scheme 1. Protons absorbing at δ 3.58$-$3.56 are coupled with those at δ 3.88$-$3.86, whereas that latter are also coupled with protons at δ $\sim$4.1 and correspond respectively to H$_{c'}$, H$_{e'}$, and H$_{d'}$.

Values of the chemical shifts of weak signals in the ^{31}P NMR spectrum between 1.3 and -0.4 ppm can be assigned to di- and triesters of phosphoric acid. The corresponding protons have the same chemical shift as protons of **2a**, which suggests that these compounds are products of an α opening of the oxirane ring. According to Biela et al., we assign the lower-field signals (0.6$-$0.2 ppm) to diesters (structure **5**) and the subsequent region (i.e., 0.1 to -0.4 ppm) to triester species.

An increase in the acid/GMA ratio results in an increase in the share of compounds **1**, **2a**, and **3**, which indicates, as might be expected for steric reasons, that GMA reacts more with H$_3$-PO$_4$ than with its esters. However, even if an excess of H$_3$PO$_4$ is used, some of the GMA molecules react with hydroxyl groups

of **2a** or **2b**, leading to the formation of **4**. ^{1}H NMR studies of oligomers obtained in the reaction of equimolar amounts of GMA and H$_3$PO$_4$ carried out at 75 °C in the DMF-d_7 solution show that about 70% of the GMA molecules participate in the addition to P$-$OH groups of H$_3$PO$_4$ and its esters, and about 30% of GMA molecules add to C$-$OH groups. The percentage of the addition of GMA to P$-$OH groups was almost the same (28%) when a 3-fold excess of H$_3$PO$_4$ is used. However, when GMA was used in excess (sample with 3 wt % of H$_3$PO$_4$), the share of C$-$OH substitution was about 50% and increased further when the measurements were repeated after 2 weeks. These results are different than those previously obtained when the reaction was carried out in DMSO-d_6, suggesting that the course of the reaction depends on the type of solvent used.

4.2. FT-IR and Raman Investigation. Interactions between the different components of the polymer gel electrolyte (i.e., polymer matrix, acid, and solvent) were examined using FT-IR and FT-Raman techniques. Such techniques have been widely applied to the investigation of molecular and ion coordination in similar systems.[4,5,7$-$9,18]

In the system of interest, PGMA$-$DMF$-$H$_3$PO$_4$, it is expected that complex interactions (exchange of protons) occur between the acid and the polymer matrix on one hand and between acidic components (H$_3$PO$_4$ and acidic groups of the polymer) and solvent on the other. To the simplify the interpretation of the spectra, the FT-IR and Raman spectra of a specially prepared series of polymer-free samples (liquid electrolytes) are compared with the spectra of polymer gel electrolyte samples with the same solvent$-$phosphoric acid composition as that of the liquid electrolytes.

The formation of the polymer is confirmed by the disappearance of the characteristic bands of the double bond (i.e., $\nu_{C=C}$ at 1637 cm^{-1} and the bands ascribed to the $=$CH$_2$ twisting (τ) and wagging (ω) modes at 942 and 816 cm^{-1}, respectively). The characteristic ring-stretching bands of the oxirane ring of glycidyl methacrylate at 1255 (Raman only) and 909 cm^{-1} are

Structure of Proton-Conducting Gel Electrolytes

J. Phys. Chem. B, Vol. 107, No. 24, 2003 **5803**
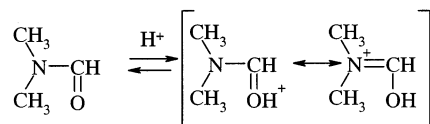
SCHEME 2: Protonation of DMF Molecules

TABLE 2: Attributes of the Most Important IR and Raman Characteristic Modes Observed in the Spectra of DMF and Perdeuterated DMF-d_7-Based Electrolytes[18,19]

mode	ν_{max}/cm^{-1}	
	DMF	DMF−H$_3$PO$_4$ complex
ν_{C-H}	2860 (IR), 2861 (R)	2870 (IR)
$\nu_{C=O}$	1675 (IR)	1659 (IR)
δ_{C-H} in-plane bending	1405 (IR), 1405 (R)	1421 (IR), 1421 (R)
γ_{C-H}	1095 (IR), 1091 (R)	1108 (IR), 1111 (R)
δ_{OCN} in-plane bending	660 (IR), 657 (R)	673 (IR), 673 (R)
$\delta_{as\ N(CH_3)_2}$ rocking	403 (R)	410 (R)
τ_{C-N}	353 (R)	370 (R)

mode	ν_{max}/cm^{-1}	
	DMF-d_7	DMF-d_7−H$_3$PO$_4$ complex
$\nu_{C=O}$	1644 (IR)	1622 (IR)
ν_{C-N}	1393 (IR), 1394 (R)	1411 (IR), 1413 (R)
δ_{OCN} in-plane bending	618 (IR), 620 (R)	636 (IR), 636 (R)
$\delta_{as\ N(CD_3)_2}$ rocking	346 (R)	349 (R)
τ_{C-N}	300 (R)	325 (R)

not present in the polymer gel sample spectra, which is further evidence for the reaction of the epoxide with the acid.

Protonation of DMF. The carbonyl group in the molecules of tertiary amides such as DMF can be easily protonated in acidic solutions (Scheme 2). As the concentration of the acid increases, a downward shift in the frequency of the stretching modes of the solvent's carbonyl groups occurs. Therefore, in the FT-IR and Raman spectra, two spectral regions are of particular interest: (a) the frequency interval between 1600 and 1700 cm^{-1} corresponding to the stretching vibration of carbonyl groups in both the solvent and the polymer matrix and (b) the spectral envelope of 630−1450 cm^{-1}, which is characteristic of different CN, CH, CNC, and CNO vibrations of solvent. The latter region is, however, more difficult to analyze because of the overlap with the characteristic bands of H$_3$PO$_4$ and ionic phosphates (1180−850 cm^{-1}). Table 2 summarizes the assignment of the most important characteristic modes for DMF and its perdeuterated analogue as well as those for the DMF−acid complex.[19,20]

Figures 6 and 7 present FT-IR and Raman spectra of the gel and liquid electrolytes with various concentrations of phosphoric acid (3−40 mass %). It is seen from Figure 6 that the increase in the acid concentration causes a shift of the $\nu_{C=O}$ peak of DMF (Figure 6a) from 1670 to 1659 cm^{-1} (Figure 6a), along with a substantial broadening of the band profile. In the Raman spectra, the peak of the carbonyl band disappears at high acid concentration (40 mass %) (Figure 7a). The unambiguously observed spectral behavior suggests a strong interaction between the solvent and acid molecules by means of the carbonyl groups. It should be stressed that this interaction not only changes the length and ordering of the C=O bonds but also affects the state of the whole solvent molecule. Thus, for example, the shift toward higher frequencies of the band at 1093 cm^{-1} (Figure 1a), attributed to the γ_{C-H} vibrations of DMF, can be attributed to the shortening of the CN bond caused by a protonation of the carbonyl groups. A similar trend is also observed for the δ_{C-N-O} vibration of DMF at about 660 cm^{-1} (Figures 6 and 7), where a downward shift and the splitting of the band is
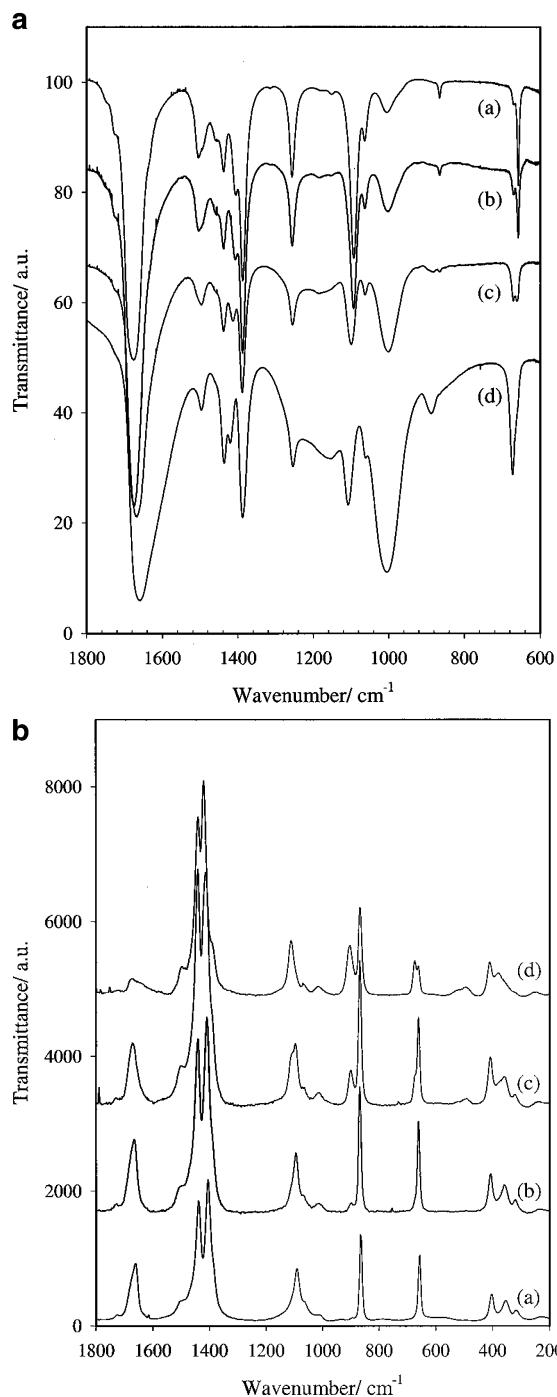

Figure 6. Comparison of (a) FT-IR and (b) Raman spectra taken for H$_3$PO$_4$−DMF solutions. The concentration of acid was equal to 3, 7, 20, and 40 wt % (curves a−d).

observed. The intensity of this component, attributed to the unprotonated form, decreases for electrolytes with higher acid concentrations. In addition, the δ_{CH} peak shows a high-frequency shift from 1405 to 1418 cm^{-1} with increasing acid concentration (Figures 6 and 7). The upward shift of the peak attributed to τ_{C-N}, from 353 to 370 cm^{-1} (Figures 7b, 8b), clearly demonstrates the strengthening and shortening of the C−N bond. Other changes such as the decrease in the intensity of the ν_{C-H} peak of the aldehyde group at higher acid concentrations and the shift of the maximum from 2860 up to ∼2880 cm^{-1} in both the IR and Raman spectra (Table 2) also support the above arguments.

Similar trends were noticed in the systems based on perdeuterated DMF (spectra not shown). For example, we observed
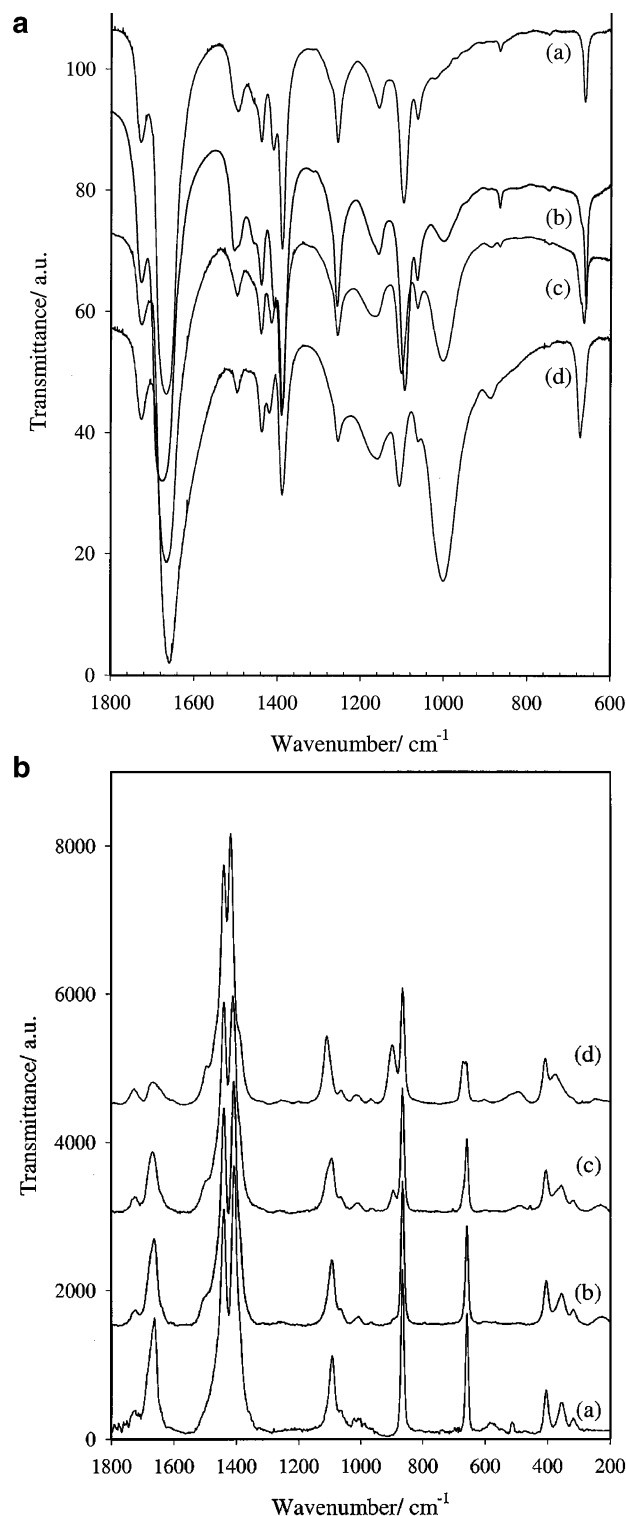
a

b

Figure 7. Comparison of (a) FT-IR and (b) Raman spectra taken for PGMA−H$_3$PO$_4$−DMF polymer gels. The concentration of acid was equal to 3, 7, 20, and 40 wt % (curves a−d, respectively).

in the gel and liquid samples the splitting of the δ_{C-N-O} vibration mode into two components, with maxima at 618 and 633 cm^{-1}. The peak of the C=O stretching vibration is broadened, and the maximum of this band is shifted from 1644 to 1623 cm^{-1}.

The analysis of the band attributed to $\delta_{N-C=O}$ gives information on the degree of protonation of the solvent molecules. The deconvolution of this peak into components related to "free" and protonated solvents (Figure 8) leads us to conclude that
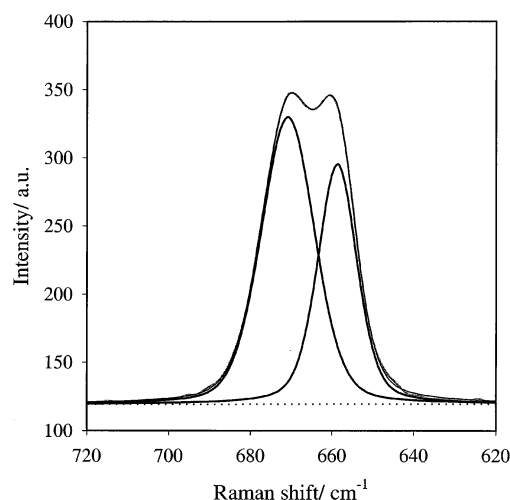

Figure 8. Deconvolution of the δ_{N-C-O} vibrational mode (Raman spectrum) of DMF for PGMA−H$_3$PO$_4$−DMF with acid content equal to 40 wt %.

TABLE 3: Dependence of Solvent Protonation on Acid Content on the Basis of the Analysis of the δ_{NCO} Vibrational Mode of DMF

acid content/wt %	percentage of protonated and nonprotonated DMF molecules	
	free	protonated
H$_3$PO$_4$−DMF		
3	~99	~1
7	93.9	6.1
20	76.2	23.8
40	39.3	60.7
PGMA−H$_3$PO$_4$−DMF		
3	~99	~1
7	94.4	5.6
20	81	19
40	42	58

the percentage of the protonated species increases almost quantitatively with the increase in acid concentration. The results of the deconvolution are collected in Table 3.

Phosphate Species Bands. In the spectra of all of the samples, it is possible to observe characteristic peaks arising from phosphoric acid. These are the P−O stretching vibrations: ν_{P-O} at 1165 cm^{-1}, $\nu_{as\ P-OH}$ at 1000−1006 cm^{-1} (Figure 7), and $\nu_{sym\ P-OH}$ at ~900 cm^{-1} (Figure 6). The intensities of these bands increase with acid concentration. The bands at ~1160 and 1180 cm^{-1} are both observed in the spectra of the liquid samples and are most likely due to the vibration of dissociated phosphate species. The absence of peaks at ~540 cm^{-1}, characterizing H$_2$PO$_4^-$ anions, suggests that the 1160 and 1180 cm^{-1} bands should be ascribed to the $\nu_{as\ P-O}$ vibration of the H$_2$PO$_4^-$ anion. This assumption is also supported by the presence of a broad band at 500 cm^{-1} (δ_{OPO} H$_2$PO$_4^-$) in the Raman spectra.[21−23] In the FT-IR spectrum of the sample with the lowest (3 wt %) acid content, there was a shoulder found at 987 cm^{-1} that most likely originated from the P(OH)$_2$ antisymmetrical PO stretch.[22,23]

In the aqueous spectra of diluted H$_3$PO$_4$, several other peaks characteristic of the H$_2$PO$_4^-$ anion are observed (e.g., the band with a maximum at 1074 cm^{-1} (PO$_2$ symmetric stretch)).[21,23] However, in the presence of DMF, this peak (PO$_2$ symmetric stretch) is completely overlapped by bands of the solvent.

The precise origin of the bands in the polymer gel samples is more difficult to assign because of the overlapping of the bands of the C−O−C, C−O−P, and phosphoric acid stretching

vibration ν_{P-O} at 1165 cm^{-1}.[24,25] The intense peak with a maximum at ~1160 cm^{-1} and a shoulder at 1170 cm^{-1} is a combination of ν_{C-O-C} of the polymer matrix and ν_{P-O-C} of the organic phosphates, which is formed in the reaction of the oxirane ring with the acid. The second band of the P$-$O$-$C stretching vibration, usually observed in the 1050$-$990 cm^{-1} region,[24,25] is unfortunately masked by the P$-$OH stretching mode at 1000$-$1006 cm^{-1}. However, at lower acid concentrations, it is possible to distinguish a weak band with a maximum at ~1018 cm^{-1}, which may be ascribed to ν_{P-O} of the alkyl ester.[25] The shoulder at ~1280 cm^{-1} appearing at higher acid concentrations in the spectra of both the liquid and the gel samples can be assigned to δ_{P-OH} of H_3PO_4 with some overlap occurring in polymer gel samples with the $\nu_{P=O}$ of the alkyl ester compounds.[22,24,25]

5. Conclusions

On the basis of ^{1}H NMR, it has been shown that in the H_3PO_4-doped polymer gels containing PGMA as a matrix most of the glycidyl groups of the polymer react with an acid. From the hetero-TOCSY and ^{31}P NMR experiments, we confirmed the presence of various phosphate species and calculated the amounts of phosphoric acid, pyrophosphoric acid, and organic phosphates and the dependence on the sample composition. As expected, gels with low acid concentration (3 and 7 wt %) contain only small amounts of pyrophosphoric acid. Most of the acid in these samples is attached to the polymer in the form of organic phosphates.

^{1}H$-^{31}$P TOCSY and ^{1}H$-^1$H COSY NMR experiments revealed that in the studied systems part of the glycidyl methacrylate reacts according to the activated monomer mechanism, leading to the formation of polyether species. These experiments showed also that for the systems with acid content equal to 3, 7, and 20 wt % most of the GMA (>60 mol %) reacts with P$-$OH groups.

The FT-IR and FT-Raman studies provide evidence of the protonation of the solvent, which increases as the acid content increases. The protonation effect is comparable for gel and liquid samples.

References and Notes

(1) Lassegues, J. C. In *Proton Conductors: Solids, Membranes and Gels—Materials and Devices*; Colomban, P., Ed.; Cambridge University Press: Cambridge, U.K., 1992; Chapter 20.

(2) Granquist, C. G. *Handbook of Inorganic Electrochromic Materials*; Elsevier: Amsterdam, 2002.

(3) Kreuer, K. D. *Chem. Mater.* **1996**, *8*, 610.

(4) Raducha, D.; Wieczorek, W.; Florjanczyk, Z.; Stevens, J. R. *J. Phys. Chem.* **1996**, *100*, 20126.

(5) Stevens, J. R.; Wieczorek, W.; Raducha, D.; Jeffrey, K. R. *Solid State Ionics* **1997**, *97*, 347.

(6) Jeffrey, K. R.; Wieczorek, W.; Raducha, D.; Stevens, J. R. *J. Chem. Phys.* **1999**, *110*, 7474.

(7) Wieczorek, W.; Żukowska, G.; Borkowska, R.; Chung, S. H.; Greenbaum, S. *Electrochim. Acta* **2001**, *46*, 1427.

(8) Żukowska, G.; Chojnacka, N.; Wieczorek, W. *Chem. Mater.* **2000**, *12*, 3578.

(9) Żukowska, G.; Wieczorek, G.; Kędzierski, M.; Florjańczyk, Z. *Solid State Ionics* **2001**, *144*, 163.

(10) Kellog, G. W. *J. Magn. Reson.* **1992**, *98*, 176.

(11) Biela, T.; Kubisa, P. *Makromol. Chem.* **1991**, *192*, 473.

(12) Biela, T.; Szymański, R.; Kubisa, P. *Makromol. Chem.* **1992**, *193*, 285.

(13) Biedron, T.; Kałużyński, K.; Pretula, J.; Kubisa, P.; Penczek, S.; Loontjens *J. Polym. Sci., Part A: Polym. Chem.* **2001**, *39*, 3024.

(14) Kreuer, K. D.; Dippel, Th.; Hainovsky, N.; Maier, J. *Ber. Bunsen-Ges. Phys. Chem.* **1992**, *96*, 1736.

(15) Bodalski, R.; Quin, L. D. *J. Org. Chem.* **1991**, *56*, 2666.

(16) Kłosiński, P.; Penczek, S. *Macromolecules* **1983**, *16*, 316.

(17) Tokar, R.; Kubisa, P.; Penczek, S.; Dworak, A. *Macromolecules* **1994**, *27*, 320.

(18) Ostrovskii, B. D.; Brodin, A.; Torell, L. M.; Appetecchi, G. B.; Scrosati, B. *J. Chem. Phys.* **1998**, *109*, 7618.

(19) Schmid, E. D.; Brodbek, E. *J. Mol. Struct.* **1984**, *108*, 17.

(20) Jao, T. C.; Scott, I.; Steele, D. *J. Mol. Spectrosc.* **1982**, *92*, 1.

(21) Adams, W. A.; Preston, C. M.; Chew, H. A. M. *J. Chem. Phys.* **1979**, *70*, 2074.

(22) Chapman, A. C.; Thirwell, L. E. *Spectrochim. Acta* **1964**, *20*, 937.

(23) Preston, C. M.; Adams, W. A. *Can. J. Spectrosc.* **1977**, *22*, 125.

(24) Bellamy, L. J. *The Infra-red Spectra of Complex Molecules*, 3rd ed.; Chapman and Hall: London, 1975.

(25) Socrates, G. *Infrared Characteristic Group Frequencies: Tables and Charts*, 2nd ed.; Wiley & Sons: New York, 1994; Chapter 17.